Real-time photoelectron spectroscopy study of the oxidation reaction kinetics on p-type and n-type Si (001) surfaces

Zhou Yu

A thesis
submitted in partial fulfillment of the
requirements for the degree of

Master of Science in Materials Science and Engineering

University of Washington
2016

Committee:

Fumio S. Ohuchi

Jihui Yang

Program Authorized to Offer Degree:
Materials Science and Engineering

University of Washington

Abstract

Real-time photoelectron spectroscopy study of the oxidation reaction kinetics on p-type and n-type Si (001) surfaces

Zhou Yu

Chair of the Supervisory Committee:
Professor Fumio S. Ohuchi
Materials Science and Engineering

Silicon oxides thermally grown on Si surface are the core gate materials of metal-oxide-semiconductor field effect transistor (MOSFET). This thin oxide layer insulates the gate terminals and the transistors substrate which make MOSFET has certain advantages over those conventional junctions, such as field-effect transistor (FET) and junction field effect transistor (JFET). With an oxide insulating layer, MOSFET is able to sustain higher input impedance and the corresponding gate leakage current can be minimized.

Today, though the oxidation process on Si substrate is popular in industry, there are still some uncertainties about its oxidation kinetics. On a path to clarify and modeling the oxidation kinetics, a study of initial oxidation kinetics on Si (001) surface has attracted attentions due to having a relatively low surface electron density and few adsorption channels compared with other Si surface direction. Based on previous studies, there are two oxidation models of Si (001) that extensively accepted, which are dual oxide species mode and autocatalytic reaction model.

These models suggest the oxidation kinetics on Si (001) mainly relies on the metastable oxygen atom on the surface and the kinetic is temperature dependent.

Professor Yuji Takakuwa's group, Surface Physics laboratory, Institute of Multidisciplinary Research for Advanced Materials, Tohoku University, observed surface strain existed during the oxidation kinetics on Si (001) and this is the first time that strain was discovered during Si oxidation. Therefore, it is necessary to explain where the strain comes from since none of previous model research included the surface strain (defects generation) into considerations. Moreover, recent developing of complementary metal-oxide-semiconductor (CMOS) requires a simultaneous oxidation process on p- and n-type Si substrate. However, none of those previous models included the dopant factor into the oxidation kinetic modeling. All of these points that further work is necessary to update and modify the traditional Si (001) oxidation models that had been accepted for several decades.

To update and complement the Si (001) oxidation kinetics, an understanding of the temperature and dopant factor during initial oxidation kinetics on Si (001) is our first step. In this study, real-time photoelectron spectroscopy is applied to characterize the oxidized (001) surface and surface information was collected by ultraviolet photoelectron spectroscopy technique. By analyzing parameters such as O 2p spectra uptake, change of work function and the surface state in respect of p- and n- type Si (001) substrate under different temperature, the oxygen adsorption structure and the dopant factor can be determined.

In this study, experiments with temperature gradients on p-type Si (001) were conducted and this aims to clarify the temperature dependent characteristic of Si (001) surface oxidation. A comparison of the O 2p uptake, change of work function and surface state between p-and n-type

Si (001) is made under a normal temperature and these provides with the data to explain how the dopant factor impacts the oxygen adsorption structure on the surface.

In the future, the study of the oxygen adsorption structure will lead to an explanation of the surface strain that discovered; therefore, fundamental of the initial oxidation on Si (001) would be updated and complemented, which would contribute to the future gate technology in MOSFET and CMOS.

Table of Contents

Chapter 1 Introduction

1.1 Applications of SiO2 Films in Semiconductor Devices

Complementary metal-oxide-semiconductor (CMOS) is a common semiconductor device that used in digital and analog circuits. It is functionalized for amplifying (deliver large load, from 10 to 50 A or more) or switching the electronic signals with little current required (less than 1mA). CMOS is composed of paired and symmetrical pairs of p-type and n-type metal oxide semiconductor field effect transistors (MOSFET) and SiO_2 is the indispensable insulating layer in MOSFET structure. [1] MOSFET has four terminals, which are gate, source, drain and substrate. Drain and source terminals are connected with the heavily doped region whilst the gate is connected to the oxide layer and the substrate terminal is connected with intrinsic semiconductor material. Since Metal-Oxide-Semiconductor (MOS) capacitor voltage can change the relative position of valence & conduction band to the Fermi-level, inversion layer will be formed between drain and source terminal. Therefore, current is able to flow through the inversion layer under an application of gate voltage. MOSFET is a voltage dependent, current output device. There are two types of MOSFET, which are n-channel and p-channel based. For n-channel, electron carries the flow on the inversion layer; for p-type channel, hole becomes the carrier of the flow. [2] In this device, the interlayer dielectric film is significant as gate materials, which work as capacitors to store charge in memory device and insulate the back-end interconnects. To meet these applications, SiO_2 had been selected as the dielectric material for the gate construction due to its low leakage current; also, it acts as a good diffusion barrier and ionic contaminants that forms a stable interface with silicon. [3]

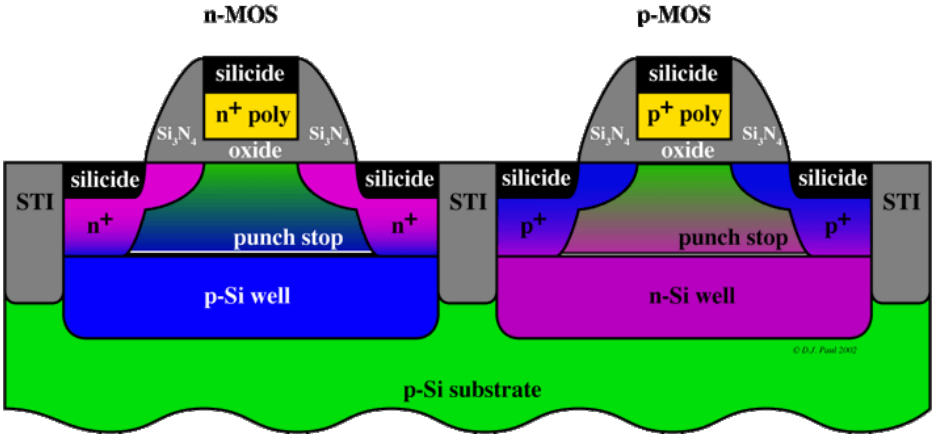

Figure 1.1 CMOS structure [21]

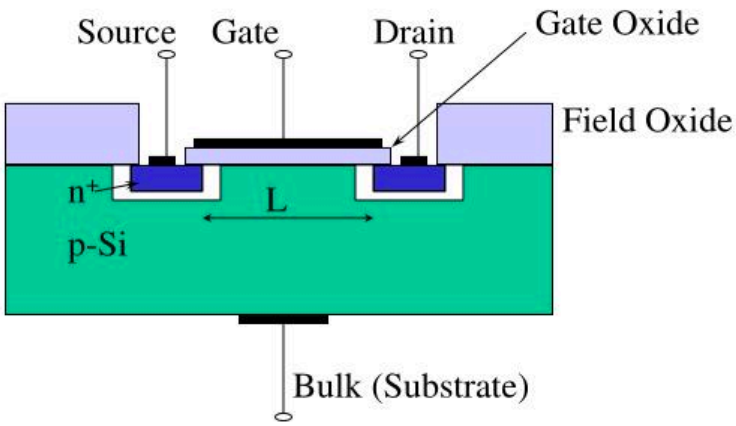

Figure 1.2 MOSFET structure [22]

1.2 SiO2 Processing Methods

Today, SiO_2 are produced in industry mainly by two oxidation processes, which are dry oxidation and wet oxidation. In dry oxidation, silicon wafer is placed under certain pressure of oxygen and oxidizes will be thermally grown on the substrate. In terms of the wet oxidation, silicon wafer is placed under a water vapor atmosphere to be oxidized. Between these two processing methods, dry oxidation is more favorable in semiconductor industry since compared with wet method, its growth rate is relatively low (<100 nm/h) and oxide layer thickness can be controlled precisely. In reverse, due to a higher oxidant solubility limit in SiO_2 of water, the wet oxidation rate is fast and it is always applied to grow thicker oxide layer. Dry oxidation is one of the key processes in semiconductor gate technology due to its growth of high quality oxide layer with monitorable layer thickness. [4]

$$Si + O_2 \longrightarrow SiO_2(dry)$$
$$Si + 2H_2O \longrightarrow SiO_2 + 2H_2(wet)$$

In dry oxidation process, furnace is the place where silicon wafers to be oxidized. In general, oxidizes will be grown under a temperature range of 700-1200 °C. Silicon wafer will be placed on a quartz boat and pushed into the center of furnace, after that, tubes deliver oxygen gas and furnace will be heated up under a programmed temperature ramp. [5] This describes the general processing conditions that semiconductor industry achieves mass production of silicon oxidizes layers on the wafer substrate.

Figure 1.3 Dry Oxidation Furnace [23]

1.3 Two Oxidation Kinetic Models Based on Previous Study

Silicon oxidation thermally grown on wafer surface is one of the crucial fabrication processes in semiconductor industry. In early 1980s, researching work was conducted on the silicon oxidation mechanism study in response of a raising demand in monitoring its growth rate and thickness. Reference on previous studies, there are two oxidation models that widely accepted, which are Duel Oxide Species and Autocatalytic Reaction Models. These two models both explain the oxidation kinetics relying on the concept of metastable oxygen atom.

1.3.1 Duel Oxide Species

This model describes the oxidation kinetic is temperature dependent and there are two oxidation growth mechanisms with a dividing temperature that locates at ~630°C. Moreover, etching of oxidation is observed when the temperature reaches >~750°C and it sacrifice those oxidation layer that previously grown. During the initial oxidation period on Si (001) surface, oxygen tends to stay on the surface as metal stable oxygen atom rather than form the stable Si-O bonded oxygen atom directly. This model proposes that under a Langmuir-type adsorption (<~630 °C), the metastable oxygen atom stays on the surface with very little diffusion as long as they arrived on the Si surface. After that, Si-O bond is formed on the surface available adsorption sites. Since the adsorption sites on the surface are limited, those saturated sites cannot accept further more oxygen atoms and this results a descending oxidation rate when time elapsed. At temperature > ~630 °C, 2D-island growth replaced the Langmuir-type adsorption and the oxygen atom is able to diffuse on the surface with sufficient thermal energy. Under the 2D-island growth, those metastable, migrated oxygen atoms tend to cluster into 2D structure (nucleation) and the adsorption of oxygen atom on Si (001) surface is in a form of oxidation layer growth, rather than

single oxygen atom adsorption growth (Langmuir-type growth). When the temperature reaches until 750°C, an etching process comes up and this consumes the surface O atom and Si atom to form SiO without forming the oxidation layer.

$$2Si + O_2 \longrightarrow 2SiO$$

Therefore, when temperature >750 °C, the etching process dominates and oxide layer is difficult to grow under a desorption of SiO. Based on this model, oxidation kinetics on Si (001) surface is temperature dependent and the diffusion kinetics of metastable oxygen atom on Si (001) surface explains the two different mechanism that divides at ~630 °C. [6]

The mathematical expression for Duel Oxide Model is in equation 1.1 where θ is the coverage of the oxidation layer surface, k_a is the adsorption coefficient and P is the the is the oxygen pressure. [7] This equation indicates that the oxidation rate is proportional to the clean surface that remained, which supports that number of available adsorption site is significant in the oxidation kinetics.

$$\frac{d\theta}{dt} = k_a P(1-\theta) \qquad 1.1$$

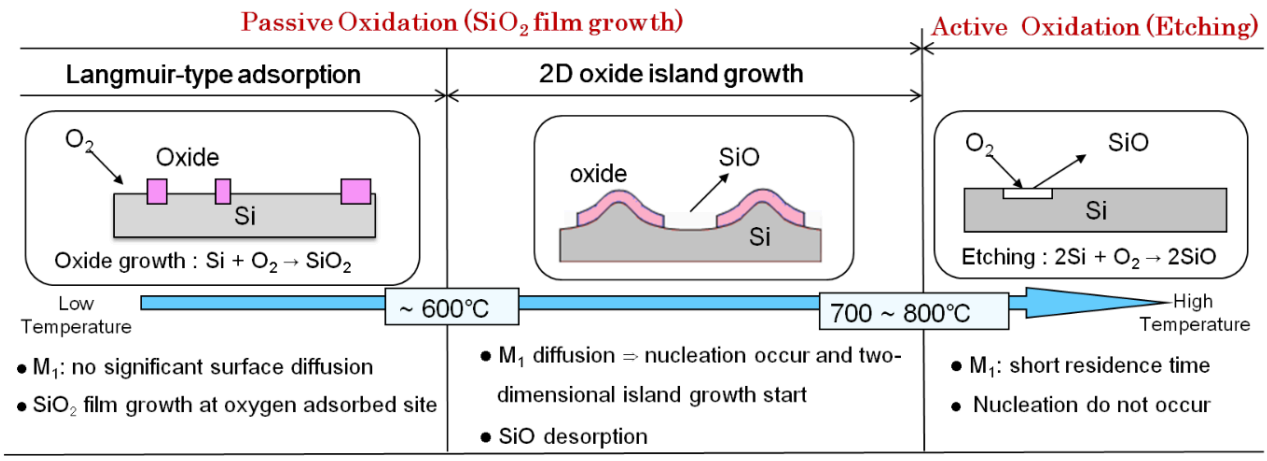

Figure 1.4 Duel Oxide Species Model [8]

1.3.2 Autocatalytic Reaction Model

The Autocatalytic Reaction Model is mainly described as the low-T Langmuir-Hinshelwood growth mode and the high T two-dimensional island growth model. They were unified and almost completely described by a single rate equation. [8] This model agrees with the previous conclusion that made in Duel Oxide Species Model, that intermediate oxygen is converted into stable oxygen that bonds with silicon site <600°C and nucleation of intermediate

oxygen contributes to the oxide growth at temperature >600°C. SiO desorption is also observed at high temperature. However, different from Duel Oxide Species model, Autocatalytic Reaction Model proposes a different mathematically expression for the kinetics. In equation 1.2, θ_0 is introduced as an indicator for this equation that for Langmuir type adsorption, θ_0>>1 and for 2D island, θ_0<<1. [7] This suggests that the oxidation kinetics can be expressed by a single equation for both kinetics into the consideration and it gives more precise evaluation on the oxidation rate.

$$\frac{d\theta}{dt} = \frac{1}{\tau_0 \theta_0}(1-\theta)(\theta_0+\theta) \qquad 1.2$$

$$\theta = \theta_0 \frac{1-e^{-kt/\tau_0}}{\theta_0 - e^{-kt/\tau_0}}$$

Though Duel Oxide Species Model and Autocatalytic Reaction Model has different mathematical evaluation on the oxidation rate of Si (001) surface, they both agree that there are two temperature dependent kinetic mechanisms that divided at ~600°C for O atom forming the oxidation layer on the surface.

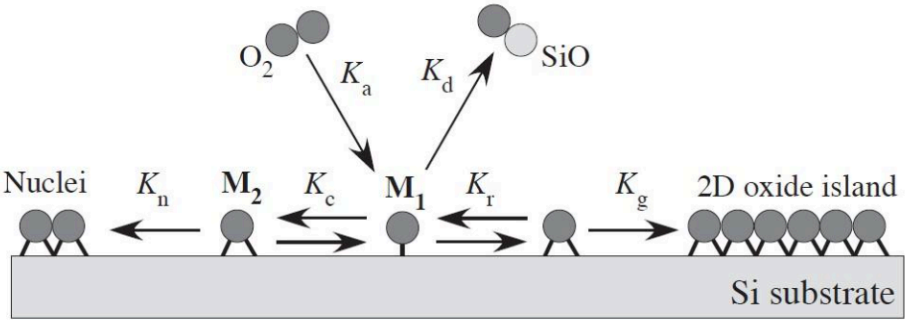

Figure 1.5 Autocatalytic Reaction Model, M1 represents metastable O atom, M2 represents stable O atom. When M1 transfer to M2 or nucleation, the adsorption coefficient (k) with different value in equation 1.2 [15]

1.4 Si (001) Surface Reconstruction

Si (001) surface has attracts researching attention mostly for two reasons, one for its mass application in electronic device fabrication; another for its relative simple surface reconstruction capability, compared with other Si surface. An after-reconstructed Si (001) has dimmer structure and this feature provides with a lower surface energy (less dangling bonds) structure that helps the study of adsorption mechanism of different material atoms. [9] For example, (a) is the Si (001) without any reconstruction, where no dimer structure on the surface. White dot represents atom on the top surface layer, black dot represent 2nd layer atom. (b), (c), (d) are examples of 2×1, p(2×1), p(2×2) reconstructed Si (001) surface. Big grey dot represents the atom stays

upward and the big white dot represents the atom stays downward. Compared with (a), unconstructed surface, (b), (c), (d) has dimer structure and (b), (c), (d) are specified by the relative dimer atom location. [10] For our experiment, the surface structure of Si (001) is reconstructed into a 2×1 structure. This dimmer structure can be understood as two top layer Si atoms are bonded together at the dimer, also with their adjacent surface atoms. In another word, we have two upward Si atoms on the top layer surface and this is our oxygen adsorption geometry.

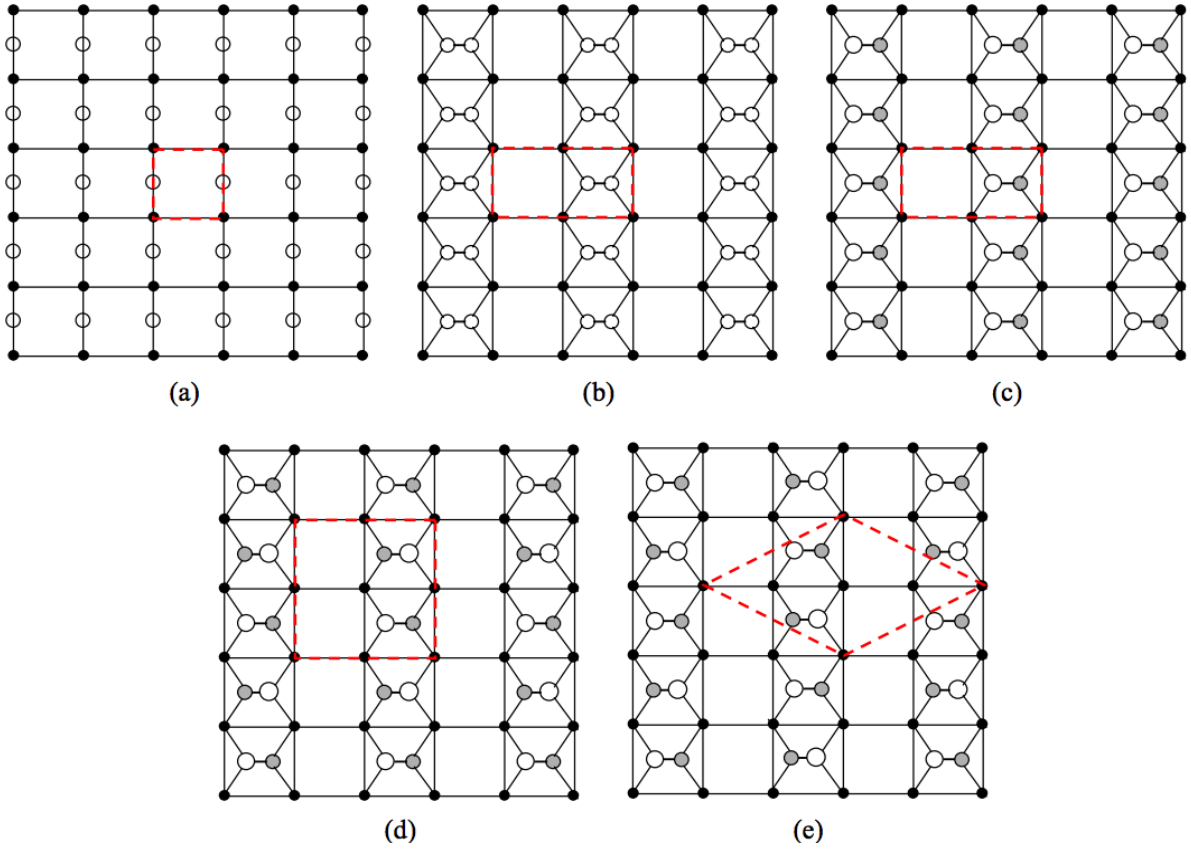

Figure 1.6 (a) unconstructed surface (b) 2×1 reconstruction (c) p(2×1) reconstruction (d) p(2×2) reconstruction (e) 4×2 reconstruction; white dot: top layer, black dot: 2nd layer, for dimmer structure, white represents upward and grey represents downward [10]

1.5 Oxygen Atom Adsorption Configuration

In terms of the oxygen adsorption structure, there are four barrieless configuration that oxygen most favorable adsorbed. They are (a) Back-Bond (BD), (b) Dimmer Bridge (DB), (c) Top of Dimer (TD), and (d) Bridge of Two Adjacent Dimers (BD). [11]

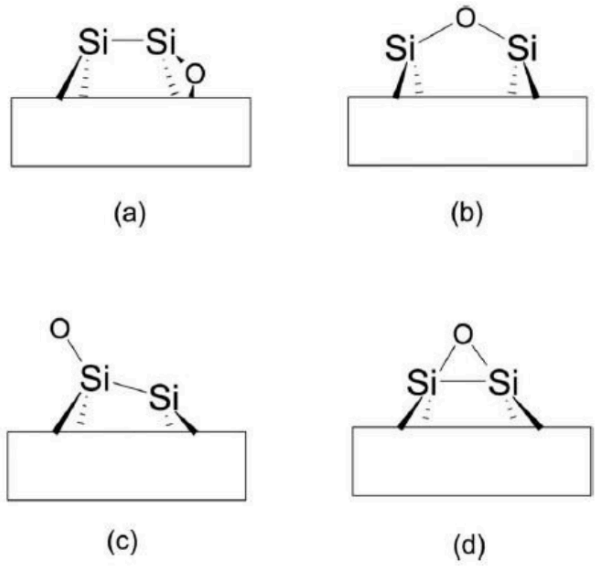

Figure 1.7 Four O atom adsorption structure (a) Back-Bond (b) Dimmer Bridge (c) Top of Dimer (d) Bridge of Two Adjacent Dimers [8]

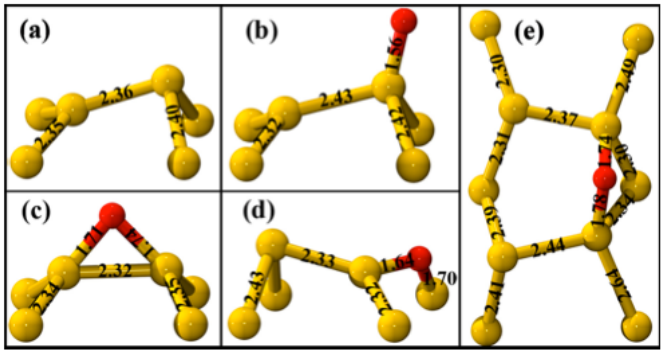

Figure 1.8 O atom adsorption structures and bond length (a) No Adsorption (b) Back-Bond (c) Dimmer Bridge (d) Top of Dimer (e) Bridge of Two Adjacent Dimer [11]

From previous research conducted on calculating the bond length and tilting angle [12], the back-bond structure was found to be the most stable structure for atomic structure and this structure is the only configuration that accompanied with breaking Si-Si bond among those four configurations. In this case, on a Si (001) 2×1 reconstructed surface, there are four possible structure that oxygen adsorbs on surface at the initial stage and back-bond structure seems to have higher chance to be formed. In Chapter 3, the adsorption structure will be identified based on our experimental data, with a consideration of dopant factor.

Chapter 2 Purpose of This Study

Professor Yuji Takakuwa's Surface Physics Laboratory, Institute of Multidisciplinary Research for Advanced Materials, Tohoku University, observed that surface strain existed during the oxidation on Si (001) and this discovery suggests that the volume expansion of oxidation can generate the point defect, which composed by emitted Si atoms and vacancies. [8] Though previous oxidation kinetics models have already provides with a view of the initial oxidation on Si (001) surface in terms of oxidation rate and adsorption structure, it has certain limitation on explaining the strain that generated during oxidation and the impact of dopant factor to the oxidation kinetics. In this case, since those emitted Si atoms and vacancies are potential ideal adsorption sites for oxygen atoms, the strain-directed effect is necessary to be supplemented into previous models. Moreover, the discovery of surface strain points to the surface electron density, which is a significant parameter, that worth to be considered in explaining the oxidation kinetics together with the adsorption structure. The last, previous models did not specify the oxidation kinetics in respect of p-, n-type of Si surface and this dopant induced electron density difference was never considered in previous Si oxidation kinetics study. With a raising demanding on monitoring the CMOS gate size and lower scale semiconductor process technology, a kinetic study of simultaneous oxidation layer growth on both n, p-type Si surface is necessary. To achieve the study purposes, experiments are designed to find and analyze the difference of the O 2p spectra, work function and surface state of n and p-type Si (001) surface to discover the relationships between the dopant factor, electron density and the corresponding oxygen atom adsorption structure. Real time ultraviolet photoelectron spectroscopy (UPS) is utilized for this study and data of O 2p peak, work function and surface state were collected at the initial stage of Si (001) oxidation to characterize the oxidation rate, oxygen adsorption structure and the dopant factor.

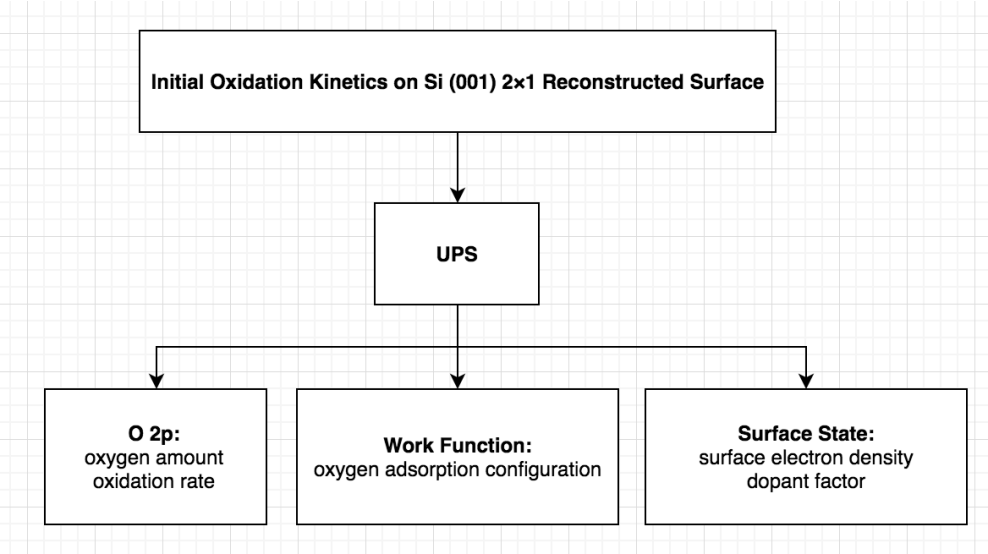

Figure 2.1 Information collected by real-time UPS experiments

Chapter 3 Experimental Methods

3.1 Experimental Technique

Experimental technique in use in this study is real-time photoelectron spectroscopy. Photoelectron spectroscopy, also known as photoemission spectroscopy, measures the electrons emitted from solids, gases or liquid by photoelectric effect to determine the binding energy of the electron on a substance. [13] In photoelectron spectroscopy, there are mainly three types of intermediates used to detect the ionization energy, which are X-ray photon, extreme ultraviolet and ultraviolet photon. Photoelectron spectroscopy relies on analysis of those ejected secondary electrons from sample surface to characterize the energy level of object surface. In this study, ultraviolet photoelectron spectroscopy (UPS) is applied to detect the molecular orbital energies in the valence region of the sample.

3.2 Integrated Surface Analysis Apparatus (RHEED-AES-UPS)

Real-time UPS experiments are conducted on the RHEED-AES-UPS comprehensive apparatus system that located at Institute of Multidisciplinary Research for Advanced Materials, Tohoku University, Sendai in Japan. This system is composed of an electron gun of reflection high-energy electron diffraction (RHEED), a helium discharging lamp, a hemispherical electron energy analyzer, a XYZ manipulator, a quadrupole mass spectrometer and a vacuum pumping system that aims to maintain the chamber with a base pressure at 1×10^{-8} pa. [8]

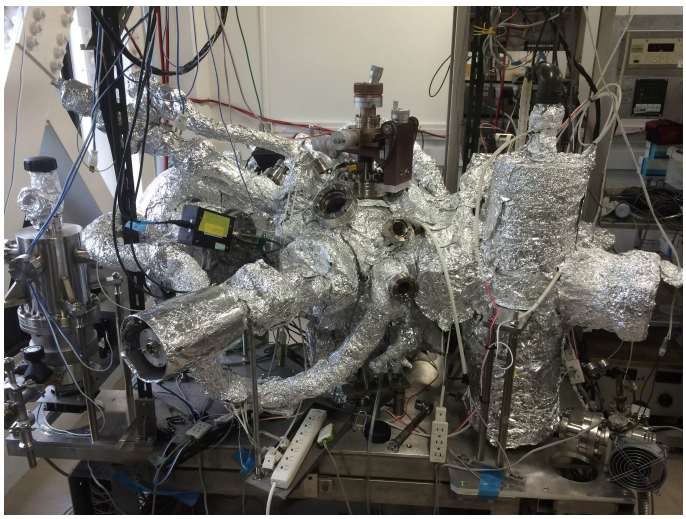

Figure 3.1 RHEED-AES-UPS system in Takakuwa lab, Tohoku University

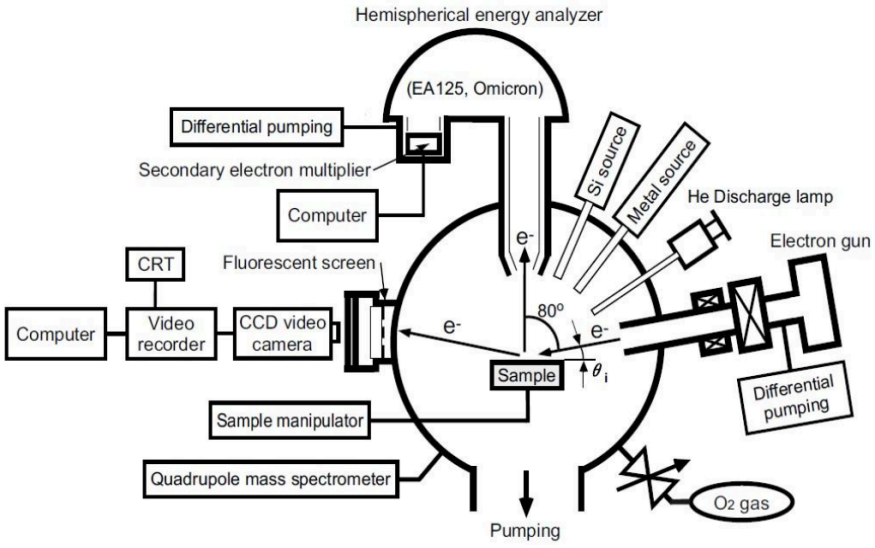

Figure 3.2 Schematic of the RHEDD-AES-UPS systems [15]

The RHEED electron gun and helium discharge lamp are pumped separately and the whole pumping system is pumped by four roughing pumps, four turbo molecular pumps and one titanium sublimation pump (TSP) that directly attached to the main chamber. The purpose of using TSP is to assist to lowering the pressure in the chamber. TSP has a titanium filament that undergoes a current of 40A periodically and this high current deliver the titanium filament reaches the titanium sublimation temperature. Since the gas phase of titanium is extreme reactive with the gas residuals left in the chamber and by this process, gas residuals are consumed and therefore pressure is reduced. [14]

The UPS unit is composed of a cold cathode noble gas discharge tube, a hemispherical electron energy analyzer and a pulse current circuit. At beginning, a He and I gas atom is initiall

ionized and then emitted free electrons that are accelerated by the electric field in the tube. Then those emitted electrons will collide with other gas atoms and this collision provides the gas atomic orbital electrons with the energy to be excited to a higher energy level. When those excited atoms falls back to a lower energy level, photon will be emitted with an energy of 21.22eV. (this value is determined by He-I resonance line ultraviolet radiation). To maintain this ultraviolet source (emitted photon), a helium gas with 11sccm flow rate and a discharging of 40 mA are applied. [15] With the ultraviolet source, generated photon will collide the sample surface and those emitted electrons from the surface will be collected and analyzed by the hemispherical electron analyzer.

The hemispherical electron analyzer (Omicron EA 125) has two concentric hemispherical electrodes. The ejected electrons will be received via the input lens, where is the place that electrons could be retarded or accelerated for different resolution inquiry. After passing through the tube, electrons will enter the hemisphere analyzer. The outer and inner sphere electrodes narrow the path energy of electrons that only for those electrons within the energy interval can arrive the detector. Whenever the analyzer received the electrons, there exist a multiplying detector and then secondary electrons are generated. These secondary electrons will be excited to a dynodes layer and positive voltage will be applied between those secondary electrons and dynodes. By generating secondary electrons, the original signals will be amplified by 10^6 times which is acceptable to be analyzed on computer software program. [16]

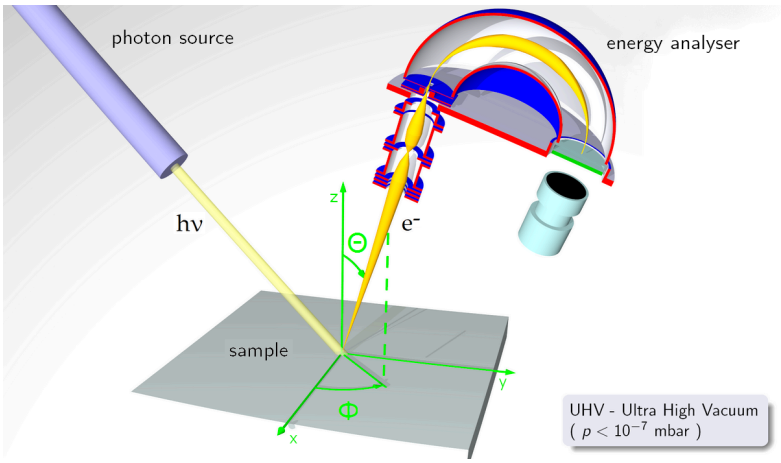

Figure 3.3 Schematic of UPS measurement [24]

In this RHEED-AES-UPS system, a customized sample heating stage makes a real-time photoelectron spectroscopy detection available. The sample (Si substrate) was heated up by charging a pulse current. Current designed as “pulsed” is for preventing the change of

trajectories of low energy secondary electron due to the magnetic field induced by direct current and the shifts of spectra due to the sample voltage. [16] To achieve the “pulse” feature, circuit is integrated with the following parts, which are gate circuit, pulse generator, heating stage, switch, dummy road, and DC power. The core fundamental of this circuits is that signal can be read as counter/time. For example, the sample heating counts to 50% of 1 ms and the signal pulse was accumulated in the 40% of 1ms. The left 10% of 1ms is designed as a time gap to avoid the decay, overshoot when switching ON or OFF of the circuit. In another word, a 10% delay in time of sample heating charge would be specified with the low energy secondary electron accumulation pulse and this makes the low energy secondary electron spectra will not affected by the real-time heating current pulse.

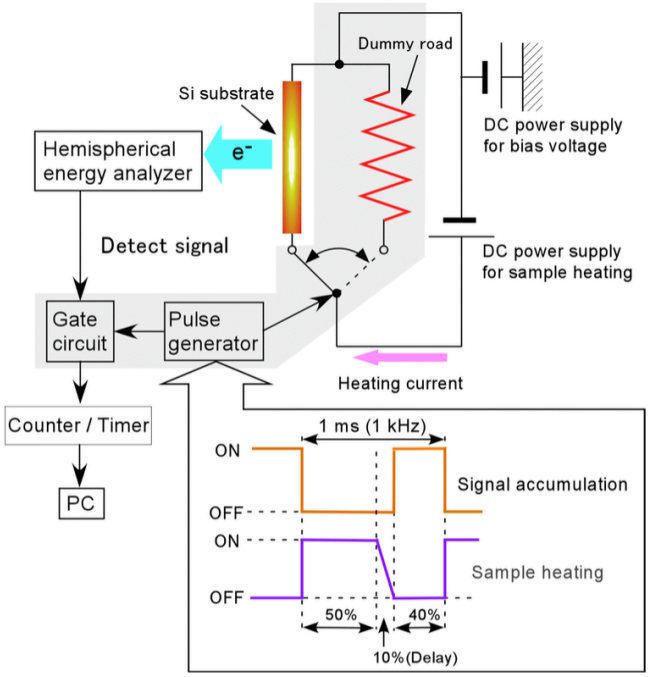

Figure 3.4 Sample heating pulse current circuit and signal accumulation system [8]

The UPS detecting angle is 45 degree between the surface normal direction for photoelectron detection and the UV light incident. Surface density is nearly 1nm depth for O2p. [8] The following spectra delivers a comparison between clean Si (001) surface and oxidized Si (001) surface that accumulated by UPS. From the spectra, there are distinguishing differences between the clean surface and oxidized surface in work function, O 2p peak and surface state.

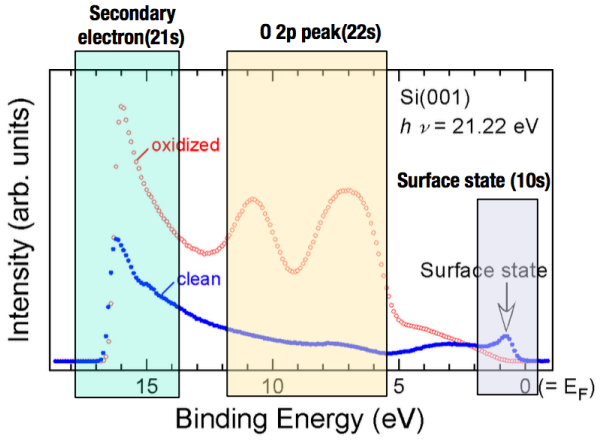

Figure 3.5 UPS spectra of cleaned and oxidized Si(001) surface. Spectra shifts observed after surface oxidized in secondary electron, O 2p and surface state peak

3.3 Sample Preparation

In this experiment, highly boron-doped p-type and arsenic-doped n-type Si (001) substrate was utilized. Size of the substrate is around 3.5×20 mm^2 and it was fixed on the sample holder with two tantalum plates. The sample-cleaning standard is RCA treatment method for preventing organic and metallic contamination. The RCA treatment process can be summarized as following:

1. Immersing the sample in acetone (C_3H_6O) and placed in supersonic cleaner for 5 mins,
2. Immersing the sample in ethanol (C_2H_5OH) and placed in supersonic cleaner for 5 mins.
3. Immersing the sample in hydrogen fluoride (HF) and placed in supersonic cleaner for 2 mins.
4. Immersing the sample in solution of hydrogen (HCl) chloride, hydrogen peroxide (H_2O_2), water in ratio of 1:1:4 for 10 minutes.

After each procedure to be done, sample was dried by N_2 gas before next step moves. Procedure 1 and 2 is work to eliminate the organic residues on the sample surface. Procedure 3 aims to remove the thin silicon oxide layer and the metallic contaminants and procedure 4 aims to form a thin oxide layer again for protecting the sample surface during transportation.

3.4 Temperature Measurement

The sample is heated by charging a pulsed current and value of that current can be adjusted by the voltage applied on the sample. Real-time measurement of voltage and current is achieved by a DC connection. Temperature of the sample is measured by an optical pyrometer. Measurement is conducted outside the chamber through the chamber window.

3.5 O_2 Pressure Measurement

The O_2 is released through the gauge valve and the gauge pressure can be adjusted. However, pressure at gauge does not represent the O_2 pressure on the sample surface. In this case, calculation of the O_2 on sample surface was conducted reference on the gauge pressure. This calculation is based on evaluating the etching rate of the Si (001) surface by RHEED intensity profiles that obtained from the recorded patterns using commercial software: (1/2, 0) and (0, 1/2) half-order spot intensity I(1/2,0) and I(0,1/2) as a measure of 2×1 and 1×2 domain. [17,18] An example of calculation result is demonstrated in figure 3.6.

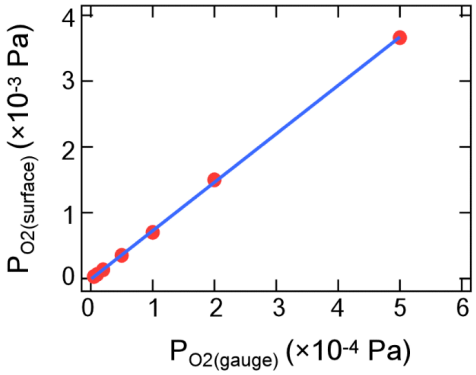

Figure 3.6 Example of calculated relationship between O_2 pressure in gauge and O_2 pressure on sample [8]

In this study, O_2 pressure on gauge is maintained at 1×10^{-5} pa, then the corresponding O_2 pressure environment of sample is $\sim4.6\times10^{-5}$ pa.

3.6 Analysis Method of Real-time UPS

UPS is mainly applied for probing the occupied electron density that closes to the surface. Therefore, ultraviolet photons with certain energy hv will shoot toward to the sample surface and then the excited surface electron energy can be analyzed to identify the density of state. Normally, ultraviolet light is illuminated by helium lamp that with 21.2 eV (He-I radiation) or 40.8 eV (He-II radiation). [19] Such a relative low photon energy suggests that photon generated from the ultraviolet source cannot penetrate into the core level, only the valence band and partial shallow core level. Therefore, this short penetration distance implies the UPS spectrum is surface sensitive that the effectively detecting depth is around 10 nm [20]. In this experiment, since the photoelectron detection angle is in 90 degrees, so the effective detecting depth is ~1 nm in reality. By using UPS, information such as density of states, valence band, secondary electron spectra and the work function can be acquired.

3.7 Analysis Method of O 2p Spectra

In this part, area under the spectra is defined as the intensity of the spectra. First spectra peak is set as the reference point and the coming new spectra data is over layered up. Since for photoelectron spectra, a background level needs to be clarified and it is set up as a line that was pulled from the beginning point of the spectra's left side to the right ending side. In another word, this line is a ground reference line that makes the peaks in spectra analyzed uniformly in intensity calculation. After that, time-evolution O 2p intensity that converted from the spectra obtained for analysis.

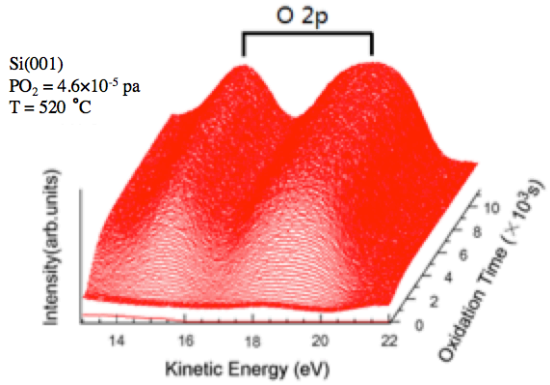

Figure 3.7 Time-evolution of O 2p spectra that collected by UPS on Si (001) surface

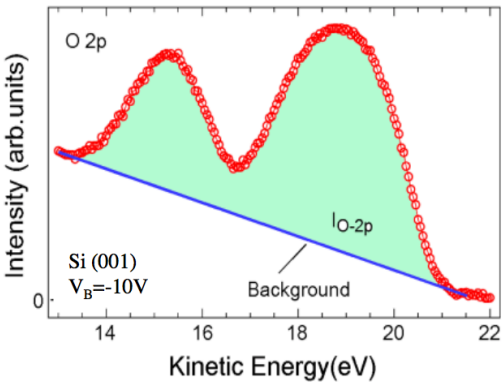

Figure 3.8 O 2p intensity area calculations beyond the reference background

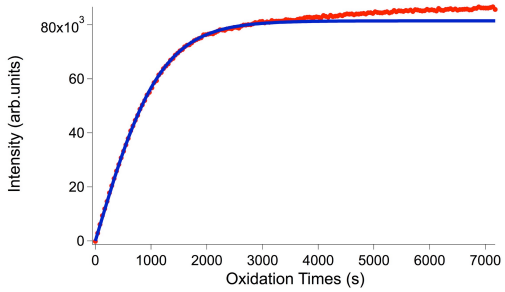

Figure 3.9 Time-evolution calculated O 2p intensity, 500°C

3.8 Analysis Method of Work Function

UPS provides with the change of work function on the target sample. Conventionally, work function is calculated as by equation 3.1 where

$$\phi = hv - E(binding\ erergy) \quad 3.1$$

Since $E\ (binding\ erergy)$ with different values for electrons in different core shell level but value of work function ϕ and UV light source hv remains stable, equation 3.1 can be modified into equation 3.2 that E_k is the kinetic energy of vacuum level and E_f is Fermi energy.

$$\phi = hv - (E_f - E_k(vacuum\ level)) \quad 3.2$$

Kinetic energy of the vacuum level E_k is determined by the low-energy cutoff of secondary electron spectra. In another word, it represents a lowest kinetic energy that secondary electron hold in vacuum level, which detected by UPS electron analyzer in a lower boundary. In terms of E_f, it represents the kinetic energy the secondary electron hold that comes from Fermi level at an infinite far position in vacuum.

For E_k, to find the exact position of low-energy cut off of the secondary spectra, least-square curve fitting is applied. Originally, the vacuum level is defined as by the step function $\mathrm{H}(E)$ that

$$\mathrm{H}(E) = \begin{cases} I_0 & (E \geq E_k(vacuum\ level)) \\ 0 & (E < E_k(vacuum\ level)) \end{cases} \quad 3.3$$

However, for the electron analyzer, it obeys the gauss function, which is

$$G(E) = \exp\left(-\frac{E^2}{\omega^2}\right) \quad 3.4$$

Basically, the kinetic energy of vacuum is determined by a convolution of the step function and gauss function that

$$I(E) = (H * G)(E) = \int_{\infty}^{\infty} H(E - x) \cdot exp\left(-\frac{(x - E_k(vacuum\ level))}{\omega^2}\right) dx \quad 3.5$$

and this equals:

$$I(E) = I_0 \int_{-\infty}^{E} exp\left(-\frac{(x - E_k(vacuum\ level))^2}{\omega^2}\right) dx \quad 3.6$$

By processing this calculation that combined with previous equation 3.4 & 3.5, the cut off position can be determined that vacuum level can be read.

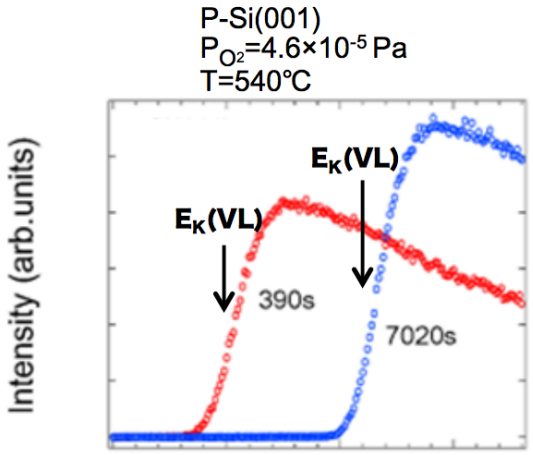

Figure 3.10 Secondary electron spectra at 390s and 7020s during oxidation on p-type Si (001) surface

In terms of E_f, it is determined by measuring the photoelectron spectrum of the Ta foil electrode for UPS. Since the electron analyzer obeys the gauss function, so the Fermi energy here is a convolution of Fermi-dirac distribution and gauss function. From the result of curve fitting, E_f = 26.19 eV. [16]

$$f(E) = \frac{1}{1+\exp\left[\frac{E-E_f}{k_B T}\right]} \tag{3.7}$$

Since E_k (vacuum level), E_f, and ultraviolet light energy hv are acquired, work function value can be calculated from equation 3.1.

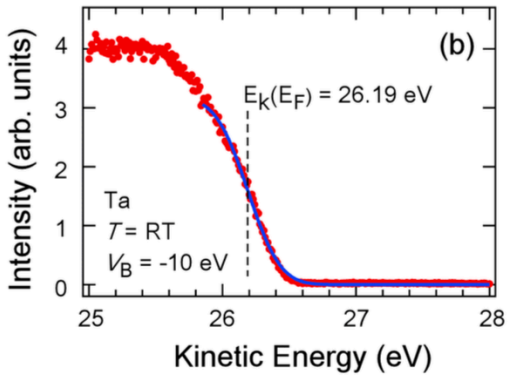

Figure 3.11 Fermi energy measurement based on photoelectron spectra [8]

Chapter 4 Results and Discussion

4.1 Saturation Level of O 2p

Saturation level of O 2p intensity was plotted in respect of oxidation time. O 2p intensity represents amount of oxygen atom adsorbs on the Si (001) substrate surface and an increasing of spectra intensity uptake curve determines an increasing amount of oxygen adsorption. Figure 4.1

summarizes results of O 2p intensity of p-type Si (001) surface under different oxidation temperature. At the beginning of oxidation, O 2p intensity climbs up and it reflects an adsorption of O atom on the surface available site. When oxidation time reaches ~2500s or later, the oxidation curve becomes stable and this suggests that available site for O adsorption has saturated and oxidation is reaching its limitation.

Based on results in figure 4.1, the oxidation saturation rate and terminal saturation level on Si (001) surface is temperature dependent that higher temperature samples demonstrate a higher ultimate O 2p intensity uptake. This indicates that under a higher temperature oxidation circumstance, amount of O atom adsorb on the surface available site is more than those samples at a relative lower oxidation temperature. For 560 °C and 580°C curves in figure 4.1, the curves climbs up gradually and both samples did not reach the saturation within a ~6000s experimental period.

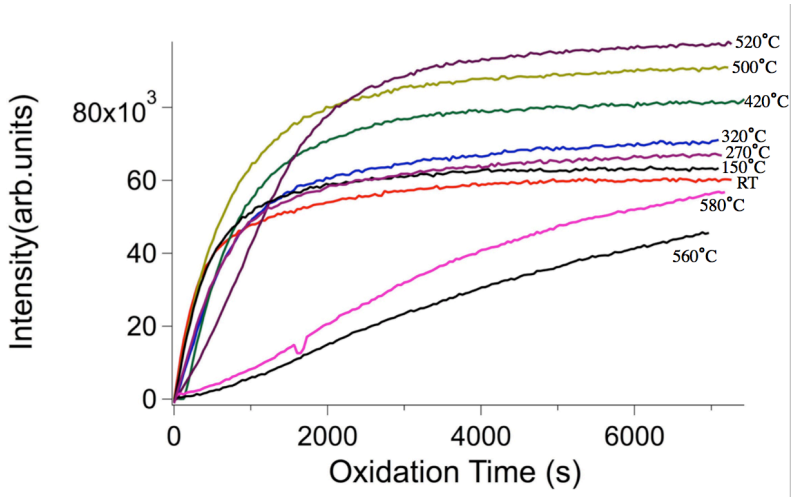

Figure 4.1 O 2p intensity on p-type Si (001) surface in temperature gradients

Therefore, beside oxidation saturation level, oxidation rate is another factor that explains the temperature dependent oxidation results. For samples with temperature <520°C, their curve slope is distinguishable larger than those samples with temperature above 560°C. In another word, sample with temperature <520°C reaches its saturation level significantly faster than those samples with temperature > 560°C, even their final saturation level is different. Based on previous study on Duel Oxide Species Model, there is a dividing point of the kinetics at ~600°C. When oxidation temperature <600°C, the oxygen tends to adsorb on the surface site directly whilst under a circumstance >600°C, oxygen atom tends to diffuse on the surface and form 2D island until oxidized. [7] Based on the O 2p result in figure 4.1, it can be predicted there exist a

dividing point between 520°C and 560°C since a difference of O 2p curve shape near the temperature interval. It partially agreed with the description from the Duel Oxide Species Mode that there exists a temperature dividing point that oxidation kinetics change on Si (001) surface. To mathematically interpret this prediction and confirm O 2p intensity curves slope are different near the temperature dividing point, Igor software was utilized to achieve curve fitting.

Two equations were used for curve fitting of O 2p intensity respectively. Reference on Duel Species Model, for sample temperature < 520°C, Langmuir adsorption type is applied whilst for temperature above 540 °C, 2D-island growth type is applied.

$$I(O\ 2p) = A_0(1 - exp(-\frac{t}{\tau})) \quad \text{Langumir adsorption} \quad 4.1$$

$$I(O\ 2p) = A_0\theta_0 \frac{1-exp(-\frac{kt}{\tau})}{\theta_0+exp(-\frac{kt}{\tau})} \quad \text{2D-island} \quad 4.2$$

For both Langmuir adsorption and 2D oxide island growth functions, A_0 represents the saturation coefficient and it is the constant that dominates the final intensity level. In this case, A_0 terms are collected from the curve fitting result for each sample curve and a plot of A_0 in respect of temperature is achieved. By comparing A_0 in corresponds with temperature, trend of oxidation saturation level can be determined under a temperature gradient. Beside the saturation constant A_0, $1/\tau$, adsorption coefficient, is parameter factor that collects from the curve fitting. $1/\tau$ determines the changing slope of intensity, which represents how fast the intensity curve reaches its saturation level.

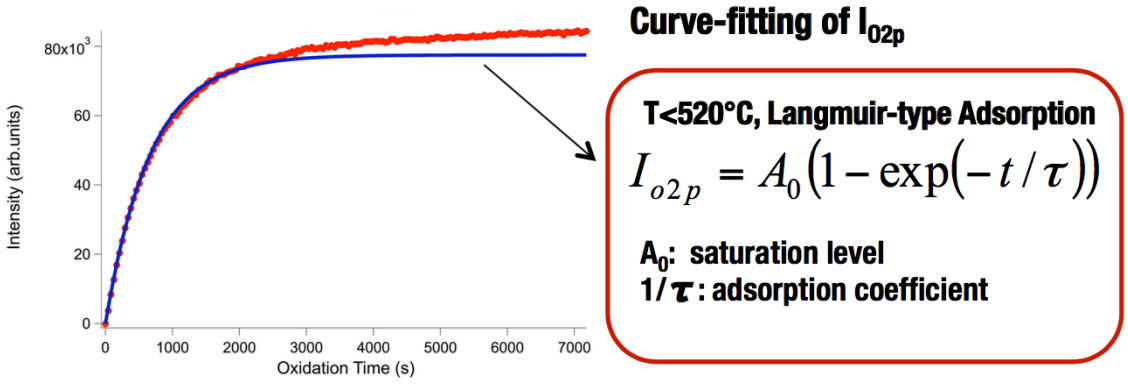

Figure 4.2 Langmuir-type adsorption curve fitting, p-type Si (001), 500°C

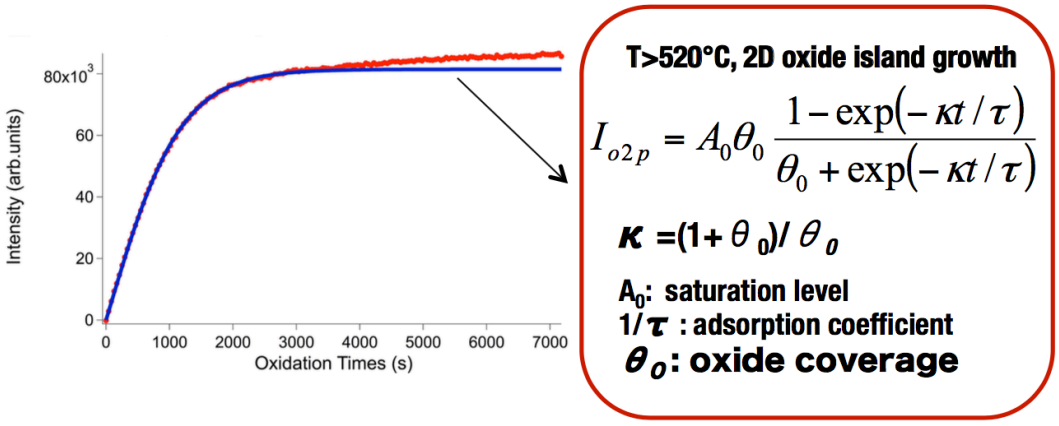

Figure 4.3 2D-island adsorption curve fitting, p-type Si (001), 540°C

In figure 4.4, saturation constant A_0 in respect of temperature is plotted and A_0 value ascends with an increase of temperature. This result indicates that when temperature <520°C, a higher temperature results a higher saturation level, which equals a larger amount of O atom attached on Si (001) surface available sites.

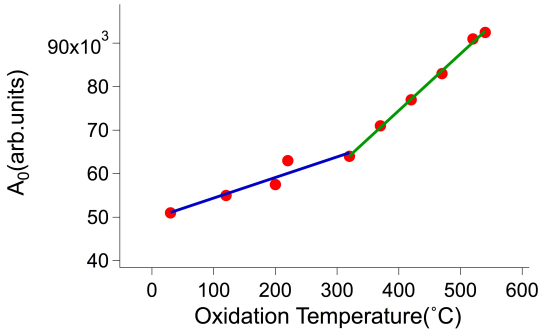

Figure 4.4 Saturation constant A_0 vs temperature on p-type Si (001)

In terms of 1/τ, adsorption coefficient, its value in respect of temperature is plotted in figure 4.5. 1/τ starts to descending from room temperature, then it remains stable within the temperature interval from 200~500°C. This suggests that when temperature <~200°C, O 2p intensity is affected by both saturation level (A_0) and adsorption coefficient (1/τ) whilst when temperature in between ~200°C to ~500°C, intensity is mainly affected by A_0 since 1/τ remains similar in this temperature region. In another word, when temperature <~200°C, an increase of temperature can boost the surface oxidation rate and final saturation level. However, when the temperature >~200°C, an increase of temperature does not boost the oxidation rate obviously and it only rise up the terminal oxygen saturation level on Si (001) surface.

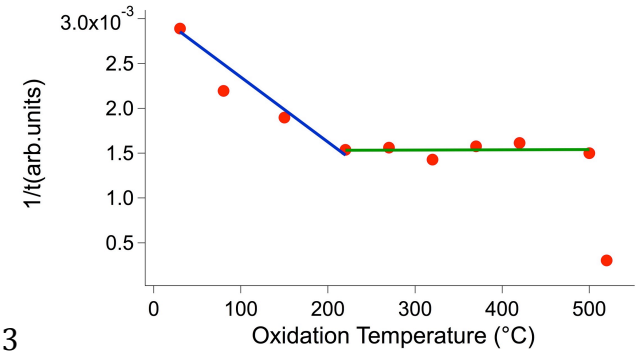

3

Figure 4.5 Adsorption coefficient 1/τ vs temperature, p-type Si (001) surface

Basically, from O 2p result, the oxidation kinetics on Si (001) surface is temperature dependent. The spectra fitting curve is determined by saturation constant and adsorption coefficient. These two parameters are temperature dependent and they dominate the O 2p spectra curve shape. The O 2p spectra in respect of dopant factor are shown in figure (4.6). Based on our results at room temperature, p- and n-type are very close in the terminal saturation level. However, n-type reaches the saturation level earlier than the p-type starting from ~500s and this suggests n-type has a relative faster oxidation after 500s. One of the possible explanation for this is n-type surface has larger free electron density on the surface and this contributes to a relative faster oxygen adsorption rate under a room temperature.

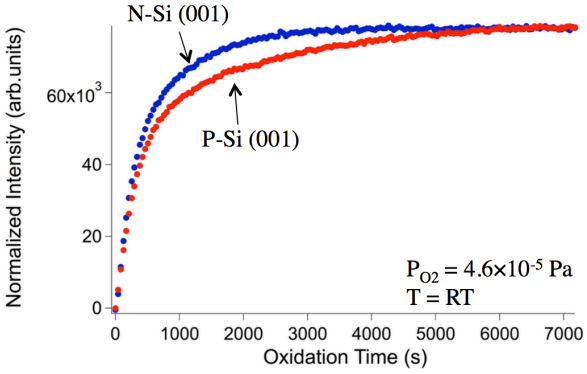

Figure 4.6 O 2p intensity on n and p-type Si (001) at room temperature

4.2 Time Evolution of Work Function

By applying real-time UPS, change of work function in respect of time is collected. The change of work function can be obtained from equation 3.2:

$$\phi = hv - (E_f - E_k(vacuum\ level)) \qquad 3.2$$

As stated in section 3.8, E_k is obtained at the secondary electron cut off position. In figure 4.7, the secondary electron cut off position at 390s and 7020s has is different and it demonstrates

that with an increasing time of oxidation, the secondary electron cutting off position is shifted. By accounting the position shift, a real time change of E_k can be achieved in respect of oxidation time.

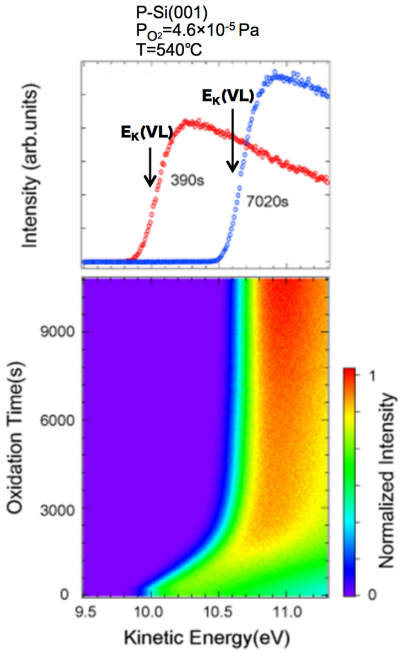

Figure 4.7 Time evolution of secondary electron cut off demonstration

In figure 4.7, time evolution of secondary electron cut off, it demonstrates that the E_k shifts to a higher intensity position with an increase of oxidation time. E_f on Si (001) surface is 26.19 eV and its value is calculated from Fermi-dirac distribution and gauss function in section 3.8. [8][16] Its value is constant and does not change with oxidation proceeded because this value represents a maximum value of kinetic energy that secondary electron can hold in the vacuum. In this case, with value of E_k and E_f, a change of work function on the experiment sample surface can be calculated based on equation 3.2. Measurement of the work function on n and p-type is conducted and this information leads to an analysis of the oxygen adsorption structure with dopant factor. (Figure 4.8)

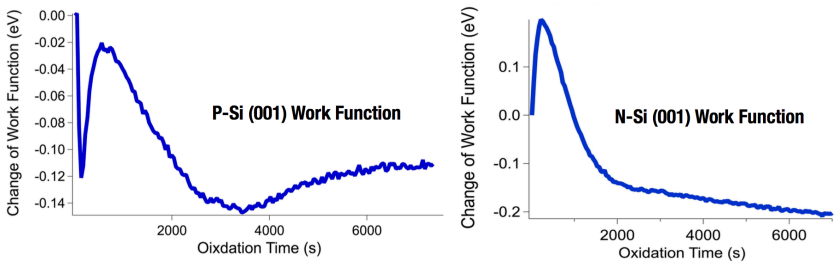

Figure 4.8 Time-evolution of work function on p-, n-type Si (001) surface, room temperature

Total change of work function of the surface $\Delta\,\phi$ equals the addition of work function change due to the surface dipole layer $\Delta\,\phi_{SDL}$ and band bending $\Delta\,\phi_{BB}$. The band bending comes from the defect generation at the oxide/Si interface and the disappearance of the surface state.

$$\Delta\,\phi = \Delta\,\phi_{surface\ dipole\ layer(SDL)} + \Delta\,\phi_{Band\ Bending(BB)} \qquad 4.3$$

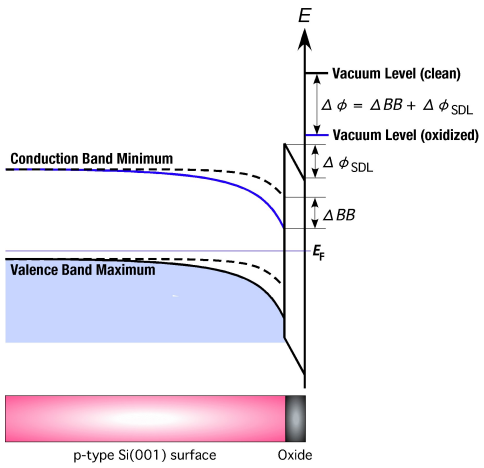

Figure 4.9 Band bending demonstration on p-type Si (001) surface

Since $\Delta\,\phi_{SDL}$ represents the change of surface dipole layer, its value change is linked to a change of O atom adsorption structure on the surface. For example, in an on-dimer structure, oxygen attaches above the surface Si site and this generates a dipole moment since O atom is more electronegativity than Si bulk. In this case, when O atom adsorbing in the on dimer structure, the oxidation surface causes an increase of $\Delta\,\phi_{SDL}$ value. Whilst for the back-bond structure, O atom breaks the Si-Si bond and it does not bond at the outermost layer of the surface. Therefore surface O atom would bond to the inner layer rather staying on outer layer surface, which causes a decrease of $\Delta\,\phi_{SDL}$ value. In this case, change of $\Delta\,\phi_{SDL}$ directly reflects the adsorption structure and its value can be calculated from $\Delta\,\phi$ and $\Delta\,\phi_{BB}$.

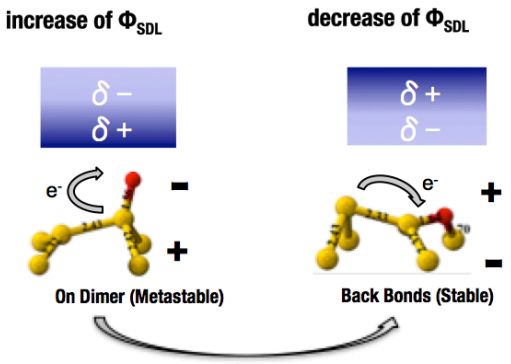

Figure 4.10 increase of $\Delta\ \phi_{SDL}$ suggests an on dimer (top of dimer) adsorption structure; decrease of $\Delta\ \phi_{SDL}$ suggests a back bond adsorption structure

Figure 4.11 demonstrates result of work function change $\Delta\ \phi$ for p-type Si (001) surface at 520°C and room temperature. To understand the relationship between $\Delta\ \phi_{SDL}$ and $\Delta\ \phi_{BB}$, analytical prediction is necessary and it is assumed that band bending $\Delta\ \phi_{BB}$ for p-type and n-type are the same under 520°C and room temperature. At 520°C, an ascending value of work function curve in respect of time represents an increase of $\Delta\ \phi_{SDL}$, which indicates a on-dimer (top of dimer) O atom adsorption structure. However, the curve approaches stable as oxidation time elapsed and this represents a saturation of O atom adsorb on the surface with on dimer structure. In addition, since the curve remains stable, $\Delta\ \phi_{BB}$ is less likely to be mainly formed since it will decrease $\Delta\ \phi_{SDL}$.

Under room temperature, spectra in figure 4.11 has a descending-ascending-descending curve shape and its the final descending curve trends suggests a negative addition of $\Delta\ \phi_{SDL}$. This represent s at room temperature, O adsorption structure is mainly back bond structure. Based on the spectra obtained at 520°C and room temperature, if we assume band bending are the same for both sample, we can conclude that on dimer structure adsorption structure dominates at 520°C whilst back bonds structure dominates at room temperature. However, this conclusion conflicts with the O_i peak result that measured by UPS. O_i peak represents O intensity in the back bond structure and if based on our assumption, O_i peak for 520°C should has less intensity than room temperature. However, from the measured result in figure 4.12, O_i intensity (back bonds level) for room temperature is weaker than 520°C sample, which completely in reverse to our predication. This conflicting result suggests that our assumption of band bending for 520°C and room temperature are the same is incorrect. In another word, it means band bending $\Delta\ \phi_{BB}$ plays a significant impact on determining the value of $\Delta\ \phi_{SDL}$ under a reference

of $\Delta\phi$. As long as $\Delta\phi_{BB}$ can be found, with knowing of the total change of work function $\Delta\phi$, $\Delta\phi_{SDL}$ can be calculated and then oxidation adsorption structure can be determined based on its changing trend in respect of time.

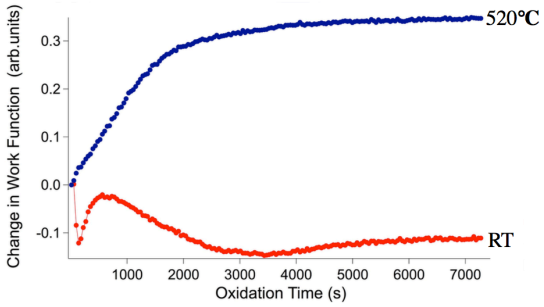

Figure 4.11 Time evolution of work function of p-type Si (001) surface at 520°C and room temperature

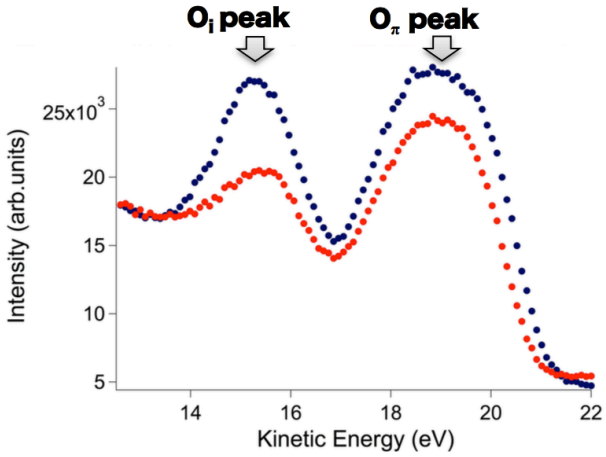

Figure 4.12 Oi peak measured on p-type sample at 520°C and room temperature, Oi peak represents O atom inserts into back bond. O_π peak represents O atom adsorbed on the surface, on dimer

4.3 Band Bending and Surface State

Value of band bending $\Delta\phi_{BB}$ in respect of time can be achieved from the measurement of surface state. When the oxygen atom adsorbs on the surface site, the dangling bonds on the surface are saturated and this leads to a change of electronic surface state and the band energy will be shifted. On the spectra data collected from UPS, oxidized surface has a surface state peak compared with the clean surface at valence band minimum. (Figure 4.13) In this case, a change of surface state equals to the value change of band energy bending $\Delta\phi_{BB}$.

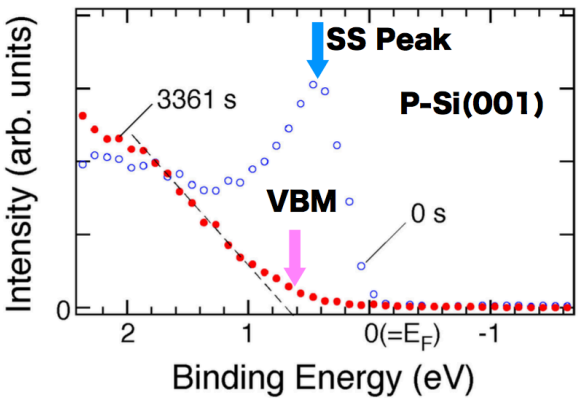

Figure 4.13 Example of comparison of valence band minimum between oxidized surface and clean surface [15]

For example, figure 4.14 represents the $\Delta \phi_{BB}$ in respect of the time on p-type Si (001) surface at room temperature and this is calculated from the change of surface state intensity that measured from UPS.

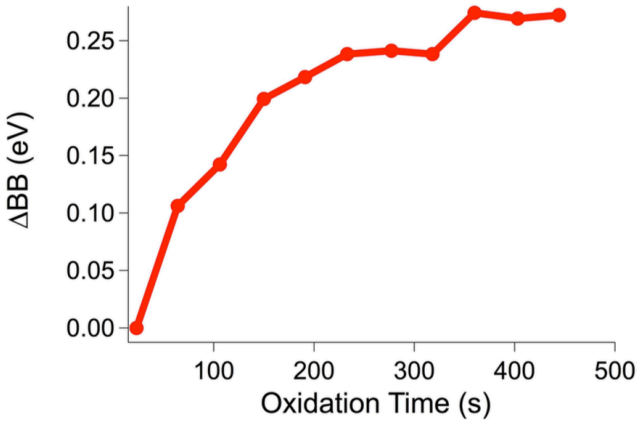

Figure 4.14 $\Delta \phi_{BB}$ calculated from change of surface state, p-type Si (001), room temperature

In this case, with change of band bending $\Delta \phi_{BB}$ and change of work function $\Delta \phi$, $\Delta \phi_{SDL}$ is calculated from equation 4.3 and its value provides us with the information about adsorption structure of O atom on Si (001) surface. Figure 4.15 demonstrates the calculation result of $\Delta \phi_{SDL}$ on p- and n-type Si (001) within the initial 500s oxidation under room temperature. Based on the result, $\Delta \phi_{SDL}$ of n and p-type Si (001) surface changing in different direction where an negative change of $\Delta \phi_{SDL}$ is observed on the p-ype surface and a positive change of $\Delta \phi_{SDL}$ is observed on the n-type surface.

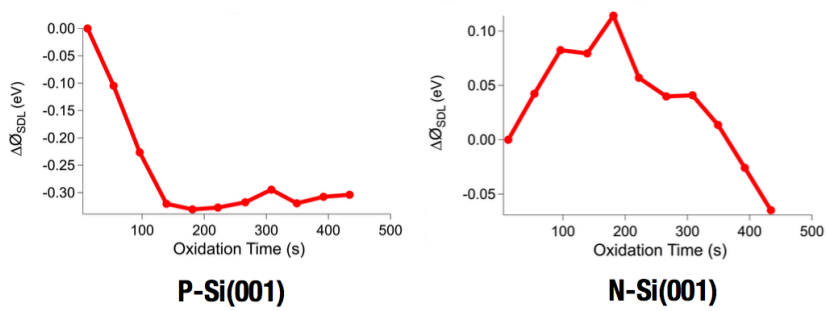

Figure 4.15Δ ϕ_{SDL} of p-, n-type Si (001) surface at initial 500s oxidation period, room temperature

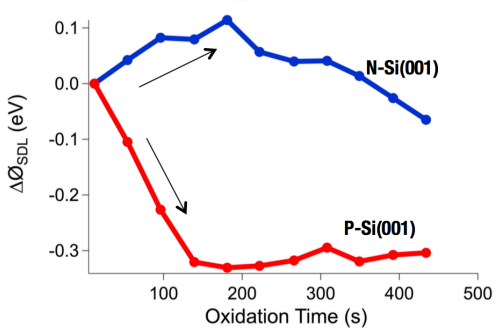

Figure 4.16Δ ϕ_{SDL} of p, n-type Si (001) surface overlay up at initial 500s oxidation period, room temperature

Since a decrease of Δ ϕ_{SDL} corresponds to a dipole moment that outer layer of surface is more positive charged than the inner layer surface, this points to a back bond adsorption structure. An increase of Δ ϕ_{SDL} points to an on-dimmer adsorption structure. In this case, it can be concluded that under a room temperature oxidation, for p-type Si (001), oxygen adsorption structure in initial oxidation is back-bond; whilst for n-type it is on dimmer.

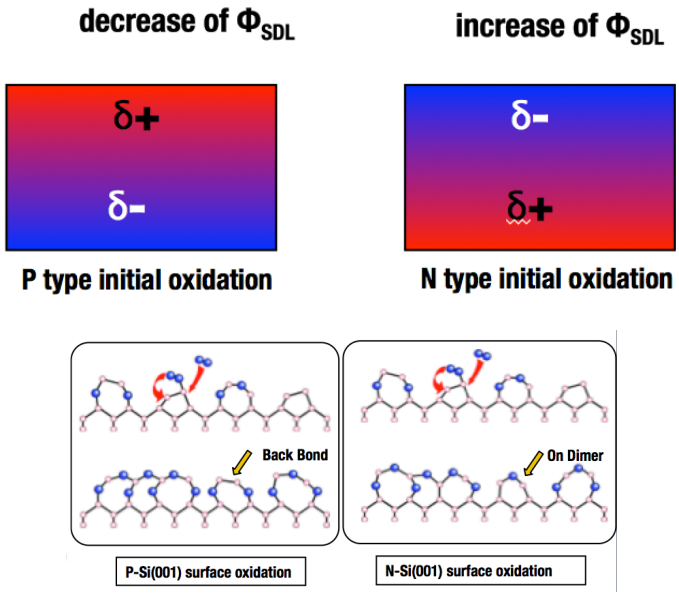

Figure 4.17 Adsorption structure demonstration of p-, n-type at initial oxidation stage, room temperature

Chapter 5 Conclusion and Future Work

In this study, ultraviolet photoelectron spectroscopy (UPS) is applied to characterize the real time oxidation surface of p- and n-type Si (001). O 2p intensity, change of work function and band bending are determined for analysis of O atom saturation level, oxidation rate and its adsorption structure on the surface. Dopant factor was introduced in this study that p-type Si (001) surface initial oxidation kinetics and n-type Si (001) surface at room temperature is discovered.

5.1 Conclusions Summarized

1. The initial oxidation kinetics on p-type Si (001) surface can be explained by Langumir model.
2. Saturation level A_0 demonstrates that p-type Si (001) oxidation is strongly temperature dependent.
3. Time evolution of work function dependent on temperature can be obtained from the secondary electron spectra of UPS. Change of work function leads to a calculation on change of surface dipole layer, which guides the determination of oxygen adsorption structure at initial oxidation.
4. Band bending of p- and n-type Si (001) surface can result a different adsorption structure at initial oxidation. For n-type, O atom attaches on the surface with a back bond structure whilst for p-type, O atom attaches with on dimer structure.

5.2 Future Work

1. O 2p spectra should be collected from the n-type Si (001) surface to confirm whether its oxidation follows the Langumir model as well and kinetic is temperature dependent.
2. Time evolution of work function and band bending measurement should cover p-, n-type Si (001) from room temperature to >600°C. This helps in mapping out the adsorption structures on p- and n-type Si (001) surface under different temperature region.
3. Further researching on the connections between adsorption structure, defect generation and corresponding strain during oxidation should be conducted to identify the mechanism of strain observed during oxidation that stated in previous study.

References

[1] R. Jacob Baker, *CMOS: Circuit Design, Layout, and Simulation, Volume 1* printed 2010. p 131, ISBN: 978-0-470-88132-3

[2] Yuhua Cheng; Chenming Hu "§2.1 MOSFET classification and operation (1999)". *MOSFET modeling & BSIM3 user's guide Springer*. p. 13. ISBN 0-7923-8575-6.

[3] Chih-Tang Sah, *Fundamentals of Solid-State Electronics, World Scientific*, first published 1991, reprinted 1992, 1993 (pbk), 1994, 1995, 2001, 2002, 2006, ISBN 981-02-0637-2. -- ISBN 981-02-0638-0 (pbk).

[4] Mircosystems Technology Laboratories SP2004 Lecture 5, *Silicon Oxidaiton*, Retrieved 22nd November 2016 from http://www.mtl.mit.edu/researchgroups/hackman/6152J/SP_2004/lectures/sp_2005_Lecture05.pdf

[5] Jaeger, Richard C. "Thermal Oxidation of Silicon". *Introduction to Microelectronic Fabrication*. Upper Saddle River: Prentice Hall. ISBN 0-201-44494-1.

[6] Y. Takakuwa and F. Ishida, "Real-Time Monitoring of the Growth and Decomposition of SiO2 Layers on Si(001) by a Combined Method of RHEED and AES", *J. Electron Spectrosc. Relat. Phenom*. 114-116 (2001) 401

[7] Maki Suemitsu, Yoshiharu Enta, Yasushi Miyanishi, and Nobuo Miyamoto, Initial Oxidation of Si (100) (2*1) as an Autocatalytic Reaction *Phys. Rev. Lett.* 82, 2334 – Published 15 March 1999

[8] Jiayi Tang, "*Study of the Formation Mechanism of SiO2 Dielectric Films for CMOS Gate Stack"*, Master Thesis (2013, Tohoku University)

[9] Chadi, D.J. (1979). "Atomic and Electronic Structures of Reconstructed Si(100) Surfaces". *Phys. Rev. Lett.* 43 (1): 43–47.

[10] Unknown Author, *Bare Si surface*, Free University of Berlin Doctor Dissertation Database, Retrieved 22nd November 2016 from http://www.diss.fuberlin.de/diss/servlets/MCRFileNodeServlet/FUDISS_derivate_000000002402/04_chapter4.pdf;hosts=

[11] Han, Han and Che, J. G., Dependence of silicon oxidation channel on distribution of surface electrons at initial stage of oxide growth on Si(001) *Applied Physics Letters*, 103, 163113 (2013), DOI:http://dx.doi.org/10.1063/1.4825366

[12] Toshihiro Uchiyama, Masaru Tsukada, Atomic and electronic structures of oxygen-adsorbed Si(001) surfaces, *Surface Science, Volume 357*, 1996, Pages 509-513, ISSN 0039-6028, http://dx.doi.org/10.1016/0039-6028(96)80076-8.

[13] IUPAC, *Compendium of Chemical Terminology*, 2nd ed. (the "Gold Book") (1997). Online corrected version: (2006–) "photoelectron spectroscopy (PES)

[14] AK Gupta, JH Leck, *An Evaluation of the Titanium Sublimation Pump, Vacuum, Volume 25, Issue 8*, 1975, Pages 362-372, ISSN 0042-207X, http://dx.doi.org/10.1016/0042-207X(75)91654-1.

[15] S. Ogawa, *"熱酸化プロセスによる極薄シリコン酸化膜形成機構の研究"*, , Doctor Thesis (2008, Tohoku University).

[16] Omicron Nanotechnology, *EA 125 Official Manual* http://uhv.cheme.cmu.edu/manuals/M470101.pdf Retrived on 22nd, Nov, 2016

[17] Y. Enta, Y. Takegawa, M. Suemitsu, and N. Miyamoto, "Growth Kinetics of Thermal Oxidation Process on Si(100) by Real Time Ultraviolet Photoelectron Spectroscopy", *Appl. Surf. Sci.* 100/101 (1996) 449.

[18] Y. Takakuwa, F. Ishida, and T. Kawawa, "Phase Transition from Langmuir-type Adsorption to Two-Dimensional Oxide Island Growth during Oxidation on Si(001) Surface", *Appl. Surf. Sci.* 216 (2003) 133.

[19] Baker A.D. and Betteridge D. *Photoelectron Spectroscopy. Chemical and Analytical Aspects.* (Pergamon Press 1972) p.ix

[20] Peter W. Atkins and Julio de Paula *Physical Chemistry* (Seventh edition, W.H.Freeman, 2002), p.980

[21] Douglas J. Paul *Complementary Metal Oxide Semiconductor* Retrieved 22nd November 2016 from http://userweb.eng.gla.ac.uk/douglas.paul/SiGe/CMOS.html

[22] Er. Vikram Kumar Kamboj *MOSFET Structure* Retrieved 22nd November, 2016 from http://www.slideshare.net/kumarsimpy/14827-mosfet

[23] Guilliaume Paumier *Furnances used for diffusion and thermal oxidaiton at LAAS Technological Facility in Toulouse, France* Retrieved 22nd November, 2016 from https://commons.wikimedia.org/wiki/File:Centrotherm_diffusion_furnace_at_LAAS_0493.jpg

[24] Saiht *General princile of ARPES with description, based on File:PES3.jpg* Retrieved 22nd November, 2016 from https://commons.wikimedia.org/wiki/File:ARPESgeneral.png

Acknowledgements

I would like to express my appreciation to Prof. Fumio S. Ohuchi for his guidance during the term of candidate. Without his valuable assistance, this work would not have been completed.

Also, I am grateful to Professor Yuji Takakuwa, who guides me to complete the experiments work during my stay in Tohoku University, Japan.

Assistant Professor Shuichi Ogawa, Doctor candidate Jiayi Tang offered generous help to my research work in Tohoku University, Japan.

Special Thanks to the following institutions. Without them, I would not have the opportunity to conduct this international cooperated study & research work in United States and Japan.

- Department of Materials Science Engineering, University of Washington
- Graduate School of Engineering, University of Washington
- Y. Takakuwa's Surface Physics Laboratory, Institute of Multidisciplinary Research for Advanced Materials
- Graduate School of Engineering, Tohoku University
- Student Exchange Division, Tohoku University